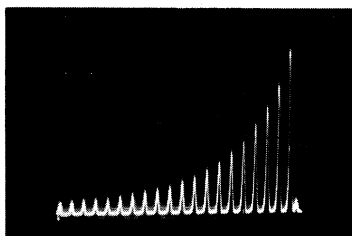


FIG. 4. Multiple reflections of longitudinal waves at 1000 Mc/sec and 15° K.



seen at 1000 Mc/sec and above. The uncertainty of the absolute values of each curve in Figs. 2 and 3 is estimated to be about 10%. The relative values are considerably more accurate, the main source of error being the calibration of the leakage signal. The frequency dependence of the attenuation is different at high and at low temperatures. Below about 25°K there is practically no variation with frequency, while above 60°K the frequency dependence appears to be between linear and quadratic. Further experiments over a wider frequency range will clarify this point.

At present we have no satisfactory explanation for our observation. It appears to be more difficult to account for the magnitude of the absorption than for its temperature dependence. It is interesting to note, in this connection, that the attenuation drops to half of its high-temperature value where the mean free path of the thermal phonons is of the same order as the acoustic wavelength, particularly in the case of transverse waves; thus this appears to be an example of interaction between sound waves and the thermal phonons. The small variation of the attenuation above this temperature may be related to the fact that here the product of the total phonon energy<sup>3</sup>  $E$  and the phonon mean free path  $l$  is nearly constant. A naive assumption of a "phonon-viscosity,"

$$\eta = E \times l / 3\bar{c}, \quad (\bar{c} = \text{average sound velocity})$$

would therefore qualitatively explain the temperature dependence, but it would account for only about 15% of the observed absorption of transverse waves above 60°K. In the case of longitudinal waves our data would, in addition, require the assumption of a considerable compressional viscosity.

Absorption due to heat conduction, as calculated for example by Lücke<sup>4</sup> and others, is one order of magnitude smaller than observed and would not account for the absorption of transverse waves.

Akhieser<sup>5</sup> and Pomeranchuk<sup>6</sup> treated the interaction between sound waves and thermal phonons in ideal crystals. Unfortunately Akhieser only

considers temperatures much higher and much lower than the Debye temperature, so that a comparison with our results is not yet possible. Pomeranchuk's results do not agree with our observed temperature dependence.

Eshelby,<sup>7</sup> Leibfried,<sup>8</sup> and Nabarro<sup>9</sup> estimated the sound absorption arising from the fact that the motion of dislocations is damped by interaction with thermal phonons. But the observed temperature dependence and the strong longitudinal absorption are difficult to understand on the basis of their models.

We should like to acknowledge gratefully very interesting discussions with C. Herring, H. J. McSkimin, and W. P. Mason of these Laboratories. We also wish to thank A. DiGiovanni for his very valuable assistance with the experiments.

<sup>1</sup>H. Bömmel and K. Dransfeld, *Phys. Rev. Lett.* **1**, 234 (1958).

<sup>2</sup>Bömmel, Mason, and Warner, *Phys. Rev.* **102**, 64 (1956).

<sup>3</sup>We are indebted to Dr. E. F. Westrum of the University of Michigan, Ann Arbor, for permission to use his data on the specific heat of crystalline quartz prior to publication.

<sup>4</sup>K. Lücke, *J. Appl. Phys.* **27**, 1433 (1956).

<sup>5</sup>A. Akhieser, *J. Phys. U.S.S.R.* **1**, 277 (1939).

<sup>6</sup>I. J. Pomeranchuk, *J. Phys. U.S.S.R.* **4**, 529 (1941).

<sup>7</sup>J. D. Eshelby, *Proc. Roy. Soc. (London)* **A197**, 396 (1949).

<sup>8</sup>G. Leibfried, *Z. Physik* **127**, 344 (1950).

<sup>9</sup>F. R. N. Nabarro, *Proc. Roy. Soc. (London)* **A209**, 278 (1951).

## RESONANCE PHENOMENA IN LARGE-ANGLE HELIUM ION-HELIUM ATOM COLLISIONS\*

F. P. Ziemba and E. Everhart  
Physics Department,  
University of Connecticut,  
Storrs, Connecticut

(Received February 16, 1959)

When He<sup>+</sup> ions are scattered from He atoms at kev energies, a small fraction of these collisions result in large-angle scattering of the incident particle. Scattered particles from this collision (and other combinations as well) have been analyzed to determine their charge state in two previous papers,<sup>1,2</sup> the data being taken at 25, 50, and 100 kev incident energies. Two interesting facts appear from the He<sup>+</sup> on He data of these

papers. Firstly, there is hardly any variation to the charge-state fractions of the scattered helium particle as the angle of scattering varies from  $1^\circ$  to  $20^\circ$ . Secondly, the fraction of neutral helium is unexpectedly higher at 50 keV than at 25 or 100 keV, indicating that this quantity must reach a maximum within this region.

A detailed investigation of this second anomaly has uncovered several resonance peaks as shown in Fig. 1. The curve  $P_0$  is the fraction of the particles scattered at  $5^\circ$  which are neutral. There are maxima in  $P_0$  at 2.7, 4.0, 5.8, 9.6, 17.5, and 43 keV, and indications of a maximum at about 250 keV. Although the data are plotted for  $5^\circ$  scattering, the curve for  $10^\circ$  scattering is coincident at energies in excess of 15 keV. At lower energies, where the analysis is to some extent a function of the scattering angle, the peaks would be shifted if the  $10^\circ$  data were plotted. The curve for  $P_2$ , the fraction scattered as  $\text{He}^{++}$ , is plotted also. This curve shows peaks at 80, 26, and 13.5 keV and is zero at lower energies. Peaks for  $P_2$  occur where  $P_0$  is a minimum. The values for  $P_1$ , the fraction scattered as  $\text{He}^+$ , are not shown but are readily found since  $P_0$ ,  $P_1$ , and  $P_2$  must add to unity.

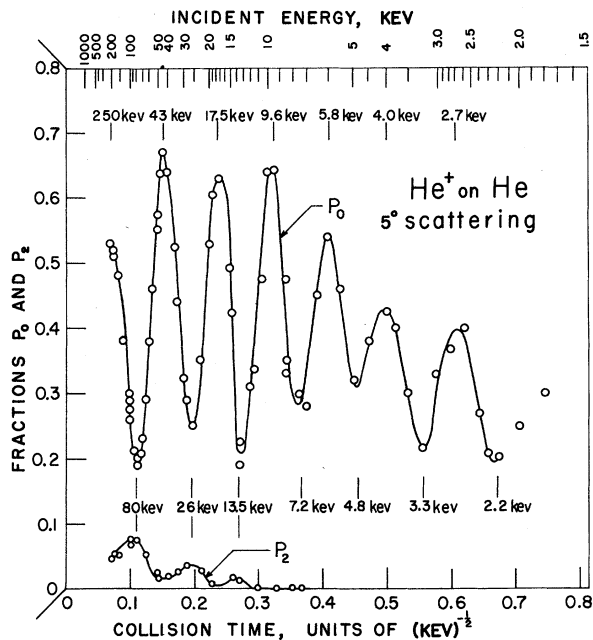


FIG. 1. The particles scattered at  $5^\circ$  from a  $\text{He}^+$  on He collision are analyzed to determine the fractions  $P_0$  and  $P_2$  which are neutral and doubly ionized, respectively. These fractions are plotted as a function of collision time on the lower axis and incident energy in keV on the upper axis. Several resonance peaks are shown.

The data are plotted on a scale spaced in proportion to the collision time, which varies as the inverse square root of the energy. It is immediately evident that the high-energy peaks are evenly spaced on this scale and there is a strong indication that the peak at about 250 keV is the first one in the series. The low-energy peaks are spaced progressively further apart.

A qualitative explanation of these phenomena may be the following: At 250 keV the collision time is so short that an electron from the neutral target atom has just time to jump to the ion and neutralize it. At 80 keV the electron has time to jump to the ion and back to its original atom. At 43 keV the electron has time to jump on and off and on again, and so on. The formation of the  $\text{He}^{++}$  is a nonresonant competing process at high energies upon which effects of the resonant capture process are superimposed.

It is most interesting that Firsov<sup>3</sup> and Massey, Bates, and Stewart<sup>4</sup> have predicted that the differential cross section for elastic scattering with charge exchange of an ion in its own gas should vary as  $\sin^2 [kE^{-\frac{1}{2}}]$ , where  $E$  is the energy and  $k$  is a constant. Our data clearly show this sort of energy dependence. However, their theories were expected to be valid at low energies, of the order of a few keV or less.

Our data were taken with essentially the same apparatus as in our previous work<sup>1,2</sup> except that the detector is now a secondary electron multiplier which counts the scattered particles individually. We have not yet developed a method of calibrating and comparing the counting efficiencies for neutrals and singly-ionized atoms below 25 keV. The heights of the peaks and depths of the valleys may need later adjustment when this calibration is made. The gradual falling off of peak heights of  $P_0$  at low energies might simply reflect a decreased efficiency in the counting of neutrals. The energies at which the peaks and valleys occur should not depend on this calibration.

We would express our thanks to Dr. Arnold Russek for valuable discussions of this phenomenon and to Mr. Grant Lockwood for his help in obtaining the data.

\* Sponsored by the Office of Ordnance Research, U. S. Army.

<sup>1</sup>Fuls, Jones, Ziemba, and Everhart, Phys. Rev. **107**, 704 (1957).

<sup>2</sup>Jones, Ziemba, Moses, and Everhart, Phys. Rev. **113**, 182 (1959).

<sup>3</sup>O. B. Firsov, J. Exptl. Theoret. Phys. (U.S.S.R.)

21, 1001 (1951).

<sup>4</sup>Bates, Massey, and Stewart, Proc. Roy. Soc. (London) A216, 437 (1953).

## ROTARY SPIN ECHOES

I. Solomon

Centre d'Etudes Nucléaires de Saclay,  
BP2 à Gif-sur-Yvette  
(Seine et Oise), France  
(Received March 9, 1959)

Torrey<sup>1</sup> has observed the free precession of nuclear spins around an rf field  $H_1$ , fixed in a frame rotating at the Larmor frequency  $\omega_0 = \gamma H_0$  around a large dc magnetic field  $H_0$ . He showed that, for an  $H_1$  much larger than the inhomogeneity of  $H_0$ , the latter has a negligible effect on the decay of the spin magnetization which is mainly due to the inhomogeneity of  $H_1$ . We report here on a method of overcoming the inhomogeneity of  $H_1$  by the production of echoes in the rotating frame ("rotary echoes") which are very similar to the usual spin echoes.<sup>2</sup> The rotary echoes, however, have some additional specific features that make them particularly suitable for the measurement of long relaxation times.

Consider the rotating frame with the  $z$ -axis along  $H_0$  and the  $x$ -axis along the rf field  $H_1$ . If at the time  $t=0$  we suppose that the spin magnetization  $M$  is along the  $z$ -axis,  $M$  will precess in the  $yz$  plane and, at  $t=\tau$ , the angle of precession is  $\phi = \gamma H_1 \tau$ . In practice  $H_1$  is inhomogeneous, with a half-width  $\Delta H_1$ , and will vary within the sample. Therefore, the total magnetization, sum of magnetization vectors at different points of the sample, will fan out in the  $yz$  plane in a time of the order of  $1/\gamma \Delta H_1$ .

At  $t=\tau$ , we perform a  $180^\circ$  phase shift on the rf field so that  $H_1$  is suddenly reversed in the rotating frame. From then on, the magnetization vector, at each point, will precess at the same rate as before, but in the opposite direction. Therefore, at time  $t=2\tau$ , the angle of precession will cancel out and all the magnetization vectors will be in phase again on the  $z$ -axis producing an "echo," as shown in Fig. 1.

In that way, we overcome the effect of the inhomogeneity of  $H_1$  and we measure only the effect of spin relaxation. For example, in a liquid where the Bloch equations<sup>3</sup> are valid, the envelope of the echoes, when  $\tau$  is varied, is an exponential curve with a time constant  $T$  given

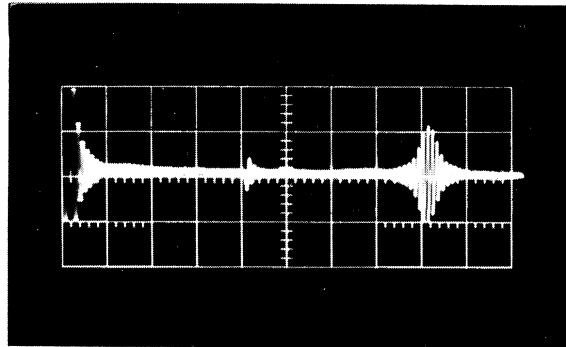


FIG. 1. A "rotary echo" in doped water. The total trace is 100 msec long.

by<sup>1</sup>

$$-\frac{1}{T} = \frac{1}{2} \left( \frac{1}{T_1} + \frac{1}{T_2} \right),$$

where  $T_1$  and  $T_2$  are the longitudinal and transverse relaxation times, respectively. The main limitation of the rotary echo method is due to self-diffusion in the liquid just as in the standard spin-echo experiment. Its effect can be greatly reduced, as in the Carr-Purcell<sup>4</sup> method, by reversing  $H_1$  (which corresponds to a  $180^\circ$  pulse in a spin-echo experiment) not only at  $t=\tau$  but also at  $t=3\tau$ ,  $t=5\tau$ , ...,  $t=(2n+1)\tau$ ; the echoes then occurring at  $t=2\tau$ ,  $t=4\tau$ , ...,  $t=2(n+1)\tau$ .

The main difficulty in applying the spin-echo method in the measurement of long relaxation times is that (a) in order to overcome diffusion a large number of  $180^\circ$  pulses must be applied, and (b) the errors on the  $180^\circ$  pulses being cumulative, a large number of pulses give poor reproductibility. A remarkable feature of the "rotary echoes" is that the errors on the reversals of  $H_1$  are not cumulative. This can be seen by a detailed analysis in the rotating frame in a manner analogous to that described by Meiboom and Gill<sup>5</sup> for their modified Carr-Purcell method. The result is the possibility of obtaining a large number of echoes (1000 are shown in Fig. 2) with good stability, while it was practically impossible to obtain in the same magnet more than 30 echoes of the Carr-Purcell type. Figure 2 shows a measurement of relaxation time in oxygen-free benzene which yields the value  $T_2 = 19.6 \pm 1.5$  sec.

We use a crossed coil spectrometer. The transmitting coil is fed by a gated oscillator giving an rf field  $H_1$  up to 1.5 gauss (rotating component). As in Torrey's experiment,<sup>1</sup> we